Published in final edited form as:
Neuropharmacology. 2010 March ; 58(3): 640. doi:10.1016/j.neuropharm.2009.11.013.

Pharmacological activity of C10-substituted analogs of the high-affinity kainate receptor agonist dysiherbaine

L. Leanne Lash-Van Wyhe[1,2], **Pekka A. Postila**[3], **Koichi Tsubone**[4], **Makoto Sasaki**[4], **Olli T. Pentikäinen**[3], **Ryuichi Sakai**[5], and **Geoffrey T. Swanson**[2]

[1]Department of Pharmacology and Toxicology, University of Texas Medical Branch, 301 University Blvd., Galveston, TX [2]Department of Molecular Pharmacology and Biological Chemistry, Northwestern University Feinberg School of Medicine, 303 E. Chicago Ave., Chicago, IL 60611 [3]Nanoscience Center and Department of Biological and Environmental Science, P.O. Box 35, FI-40014, University of Jyväskylä, Finland [4]Laboratory of Biostructural Chemistry, Graduate School of Life Sciences, Tohoku University, Aoba-ku, Sendai, Japan [5]Faculty of Fisheries Sciences, Hokkaido University, Hakodate 041-8611, Japan

Summary

Kainate receptor antagonists have potential as therapeutic agents in a number of neuropathologies. Synthetic modification of the convulsant marine toxin neodysiherbaine A (NDH) previously yielded molecules with a diverse set of pharmacological actions on kainate receptors. Here we characterize three new synthetic analogs of NDH that contain substituents at the C10 position in the pyran ring of the marine toxin. The analogs exhibited high affinity binding to the GluK1 (GluR5) subunit and lower affinity binding to GluK2 (GluR6) and GluK3 (GluR7) subunits in radioligand displacement assays with recombinant kainate and AMPA receptors. As well, the natural toxin NDH exhibited ~100-fold selectivity for GluK2 over GluK3 subunits, which was attributable to the C8 hydroxyl group in NDH. We used molecular dynamic simulations to determine the specific interactions between NDH and residues within the ligand-binding domains of these two kainate receptor subunits that contribute to the divergent apparent affinities for the compound. These data demonstrate that interactions with the GluK1 subunit are preserved in analogs with substitutions at C10 in NDH and further reveal the determinants of selectivity and pharmacological activity of molecules acting on kainate receptor subunits, which could aid in design of additional compounds that target these receptors.

Keywords

glutamate receptor; marine natural product; synthetic; radioligand binding; electrophysiology; ligand-binding domain

Correspondence to: Geoffrey T. Swanson, Ph.D., Department of Molecular Pharmacology and Biological Chemistry Northwestern University Feinberg School of Medicine, 303 E. Chicago Ave., Searle 7-443, Chicago, IL 60611, Tel: (312) 503-1052; Fax: (312) 503-1402 gtswanson@northwestern.edu.
Reprint requests: Geoffrey T. Swanson, Ph.D., Department of Molecular Pharmacology and Biological Chemistry, Northwestern University Feinberg School of Medicine, 303 E. Chicago Ave., Searle 7-443, Chicago, IL 60611, Tel: (312) 503-1052; Fax: (312) 503-1402 gtswanson@northwestern.edu

INTRODUCTION

Understanding the diverse functional roles played by kainate receptors in the mammalian central nervous system will require development of new pharmacological agents. Most existing kainate receptor agonists and antagonists act either non-selectively or preferentially on receptors containing the GluK1 (formerly GluR5) subunit (Jane et al., 2008), and some selective antagonists show therapeutic potential in preclinical animal models of pain and other neuropathologies (Jane et al., 2008). Further insight into the molecular interactions between selective ligands and residues within the receptor subunit ligand-binding domains (LBDs) could guide future synthetic efforts at generation of molecules selective for the other kainate receptor subunits, GluK2 (GluR6), GluK3 (GluR7), GluK4 (KA1), and GluK5 (KA2).

The natural marine excitotoxins dysiherbaine (DH) and neodysiherbaine A (NDH) serve as useful scaffolds to explore such molecular interactions. Both DH and NDH were isolated from the marine sponge *Lendenfeldia chodrodes* and are potent convulsants with a high apparent binding affinity for GluK1 receptors (Sakai et al., 1997; Sakai et al., 2001a). They contain a shared structural template, consisting of a functionalized perhydrofuranopyran bicyclic ring containing a backbone of L-glutamate. Two functional groups at the C8 and C9 ring positions are important for activity and selectivity at (*S*)-α-amino-3-hydroxy-5-methyl-4-isoxazolepropionic acid (AMPA) and kainate receptors (Lash et al., 2008; Sanders et al., 2005). Removal of these substituents profoundly alters pharmacological activity, converting high-affinity agonism into a selective antagonism of GluK1 receptors (Sanders et al., 2005). Epimerization of chiral centers within the glutamate backbone of NDH also produced an antagonist, 2,4-epi-NDH, with selectivity for both GluK1 and GluK2 receptors (Lash et al., 2008). Thus, the unique structures of DH and NDH serve as useful lead compounds from which to develop additional analogs with distinct pharmacological profiles.

Here we describe the pharmacological properties of a new set of NDH analogs containing substitutions at the C10 ring position, a site on the template molecule that has not been explored to date (Sasaki et al., 2006). As with other related molecules, the C10 analogs preferentially bound GluK1 subunits with high affinity relative to other kainate receptor subunits. Intriguing differences in affinity for GluK2 and GluK3 predominantly arose in part from the functional group at the C8 position, which led us to discover that the parent compound, NDH, itself exhibited a striking divergence in affinity for these two receptor subunits. Non-conserved residues and subtle rearrangement of hydrogen bonds within the ligand binding domains of GluK2 and GluK3 could account for the subunit selectivity of NDH. These studies offer new insight into the determinants of ligand specificity within different kainate receptor subunits.

MATERIALS AND METHODS

Molecular Biology and Nomenclature

Site-directed mutagenesis of GluK2 and GluK3 cDNAs was performed using the QuikChange site mutagenesis protocol (Stratagene, La Jolla, CA). All mutant cDNAs were sequenced in full at the Northwestern University Genomics Core Facility. Kainate receptor splice isoforms used in this study were rat GluK1–2a, GluK2a, and GluK3a (GluR5–2a, GluR6a and GluR7a). AMPA receptor subunits were rat GluA1(flip) and GluA2 (flip). Amino acids are referred to using single-letter codes in the physiology and binding assays for the sake of brevity, whereas the three-letter code was used when referring to the modeling results, to be consistent with prior studies.

Cell Culture and Electrophysiology

HEK-293-T/17 cells were maintained and transfected as described previously (Lash et al., 2008). Cells were transfected with receptor cDNAs (0.05–0.2 μg) in combination with enhanced green fluorescent protein (eGFP) using the TransIT-LT1 transfection reagent (Mirus, Madison, WI) according to the manufacturer's protocol. External recording solution contained 150 mM NaCl, 2.8 mM KCl, 2 mM $CaCl_2$, 1 mM $MgCl_2$, and 10 mM HEPES, at pH 7.3. Thick-walled borosilicate glass electrodes (Warner Instruments, Hamden, CT) were pulled to a final resistance of 1.5 to 2.5 MΩ and were filled with internal solution containing the following: 110 mM CsF, 30 mM CsCl, 4 mM NaCl, 0.5 mM $CaCl_2$, 10 mM HEPES, and 5 mM EGTA, at pH 7.3. Drugs were applied rapidly through a three-barreled glass flow pipe mounted on a piezo-bimorph. Glutamate-evoked currents from transfected cells lifted into the laminar solution flow had a 10–90% rise-time of 0.8 – 1.5 ms. Whole-cell voltage-clamp recordings were carried out using an Axopatch 200B amplifier (Molecular Devices, Sunnyvale, CA). Data were analyzed with Origin 7.5 (OriginLab Corp., Northampton, MA), and Prism4 (GraphPad Software Inc., La Jolla, CA); inhibition-response curves were plotted and fit with a one-site competition curve constrained to fixed minima (0) and maxima (100). Time constants of recovery were determined by an exponential fit of recovery data.

Modeling and Molecular Dynamics Simulations

Ligand structures—The 3D structures of ligands were built with SYBYL 7.3 (Tripos, Inc., St Louis, MO) and geometry-optimized quantum mechanically with GAUSSIAN03 (Gaussian Inc., Wallingford, CT) at the HF/6–31+G* level with the continuum water (PCM) model. The atom-centered point charges were created from the electrostatic potentials (GAUSSIAN03; HF/6–31+G*) using RESP methodology (Bayly et al., 1993; Cieplak et al., 1995; Cornell et al., 1993). The charges of chemically comparable atoms in the ligands were set to identical values.

Protein structures—The 3D dimer structures of the GluK1-ligand binding core (LBC) (PDB-code: 1YCJ) (Naur et al., 2005) and the GluK2-LBC (PDB-code: 1S7Y) (Mayer, 2005) in complex with L-glutamate were obtained from the PDB. The closed GluK3-LBC monomer structure was built based on the alignment of the B chain of 1YCJ and the human GluK3 sequence (GRIK3) (Puranam et al., 1993) using MALIGN in the BODIL modeling environment (Lehtonen et al., 2004) and NEST in JACKAL 1.5 (accessible online).

Ligand docking—The ligands were docked flexibly into the GluK1-LBC with GOLD3.1.1 (Jones et al., 1995; Jones et al., 1997) into a predefined search area of a 15 Å radius sphere centered at the O^{OH}-atom of Tyr489 (GluK1 numbering used) in the ligand-binding site, otherwise default values were used. The ligand poses for MD simulations were selected based on two criteria: (a) a fitness value given by GOLD, and (b) similarity of the conformation to that observed for DH in the crystal structure of GluK1-DH complex (Frydenvang et al., 2009). The docked ligands were included in GluK2- and GluK3-LBCs by superpositioning the ligand-GluK1 docking results using BODIL to assure the same initial conformation. To accommodate 8-desmethyl-10-HM-DH into the GluK2-LBC, the side chain of Asn721 was adjusted by using the side chain rotamer library (Lovell et al., 2000) incorporated within BODIL. Side chain adjustments of Glu738 and Asn721 were also necessary for 8-desmethyl-10-HM-DH positioning into the GluK3-LBC.

Starting structures for molecular dynamics simulations—After docking of ligands and prior to the molecular dynamics (MD) simulation, water molecules located in a 1.4 Å radii around the ligands were removed from the crystal structures. Protonation of histidines were determined based on the possible hydrogen bonds with adjacent residues and water molecules in the initial protein structure. The Gly545-Thr546 artificial linker used in the crystallization

process to connect the S1 and S2 segments of the LBC was removed from all chains to allow free domain movement. TLEAP in ANTECHAMBER-1.27 (Wang et al., 2006) was used to (a) set the force field parameters for the protein (parm99) and ligands (gaff), (b) add hydrogen atoms, (c) neutralize the LBC-ligand complex with chloride or sodium ions, (d) solvate the system with a rectangular box of transferable intermolecular potential three-point water molecules (TIP3P) 13 Å in all directions, and (e) to add disulphide bridges.

Molecular dynamics simulations—The constructed LBC-ligand complexes were used as starting structures for the MD simulations. The two-step energy minimization, MD equilibration, and free MD simulation were run with NAMD 2.6 (Phillips et al., 2005). Firstly, the water molecules, counter-ions, and amino acid side chains were minimized with the conjugate gradient algorithm (15,000 steps) as the C^{α}-atoms were restrained into their initial positions with the harmonic force of 5 kcal mol^{-1} $Å^{-2}$. Secondly, the whole complex was minimized without constraints (15,000 steps) to assure complete equilibration of the system. The MD equilibration was done in constant temperature with restrained C^{α}-atoms (180,000 steps). The production simulation was performed without constraints in constant temperature and pressure for 14 ns for all ligands in complex with the LBC. All ligand-LBC complexes were simulated once.

The simulated complexes were held at constant temperature of 300 K with Langevin dynamics for all non-hydrogen atoms, using a Langevin damping coefficient of 5 ps^{-1}. A constant pressure of 1 atm was upheld by a Nosé-Hoover Langevin piston with an oscillation timescale of 200 fs and a damping timescale of 100 fs. An integration time step of 2 fs was used under a multiple time stepping scheme (Schlick et al., 1999). The bonded and short-range interactions were calculated every time step and long range electrostatic interactions every third step. A cutoff value of 12 Å was used for the van der Waals and short-range electrostatic interactions. The MD equilibration and constraint-free simulation were conducted under the periodic boundary conditions with the full-system, and the long-range electrostatics were counted with the particle-mesh Ewald (PME) method (Darden et al., 1993; Toukmaji et al., 2000). The bonds involving hydrogen atoms were restrained by the SHAKE algorithm.

Snapshot structures were extracted from the MD trajectories at 360 ps intervals with PTRAJ 6.5 (available online); the structures at the ~14 ns timepoint were utilized to represent the protein-ligand complexes.

Radioligand binding

Membrane preparations from HEK-293-T/17 cells were prepared and used in radioligand binding assays as described previously (Sanders et al., 2005). Unlabeled analogs were used to displace [^{3}H]kainate (10–20 nM, PerkinElmer Life and Analytical Sciences, Boston, MA) or [^{3}H]AMPA (20 nM, PerkinElmer Life and Analytical Sciences, Boston, MA) from kainate and AMPA receptors, respectively. The GluK4 subunit was not included in the analysis because we were unable to establish conditions that yielded specific binding to the radioligand. Nonspecific binding was determined in the presence of 1 mM glutamate. After 1 h incubation at 4°C, samples were harvested by rapid filtration onto Whatman GF/C membranes. Upon addition of scintillation fluid, membranes were incubated for 1 h at room temperature. A Beckman LS5000TD scintillation counter was used for quantification (Beckman Coulter Inc., Fullerton, CA). Data were plotted and fit with a one-site competition curve with fixed minima and maxima using Prism 4 (GraphPad Software, Inc). K_is were calculated with the Cheng-Prusoff equation using IC_{50} values derived from the fitted data and the radioligand K_d values. Saturation experiments with varying concentrations of [^{3}H]kainate (1 – 600 nM) were performed under the same conditions as above. These data were plotted and fit with a one-site binding hyperbola curve using Prism4 (GraphPad Software, Inc) to determine the radioligand

K_d values for receptors and mutants as follows: GluK2, 13 nM; GluK2(Y443F), 30.9 nM; GluK2(A518T), 5.0 nM; GluK2(Y443F/A518T), 7.6 nM; GluK3, 53.8 nM; GluK3(F446Y), 65.8 nM; GluK3(T520A), 186 nM; GluK3(F446Y/T520A), 121 nM.

RESULTS

The effect of substitutions at the C10 position of DH and NDH on pharmacological activity and subunit specificity were explored with three novel analogs (Sasaki et al., 2006). The structures of these analogs, 10-hydroxymethyl-neodysiherbaine (10-HM-NDH), 8-desmethyl-10-hydroxymethyl-dysiherbaine (8-desmethyl-10-HM-DH), and 10-methoxymethyl-neodysiherbaine (10-MOM-NDH), are shown in Figure 1 along with their parent molecules DH and NDH (carbons are numbered in DH for reference). Note that 8-desmethyl-10-HM-DH and 10-HM-DH differ only in the substituent at the C8 position, whereas 10-HM-NDH differs from 10-MOM-NDH solely in the addition of an extra methyl group to the C10 substitution.

C10 analogs exhibit highest affinity for GluK1 subunits

The radioligand binding profiles of the C10 analogs were compared to their parent compounds DH and NDH, which bind with low nanomolar affinity to a subset of kainate receptor subunits (Table 1) (Sanders et al., 2005;Swanson et al., 2002). [^{3}H]AMPA or [^{3}H]kainate was displaced from transfected HEK-293-T/17 cell membranes with a range of analog concentrations. Fitting of the data yielded IC_{50} values that were used to calculate K_i values (Table 1). Figure 2 shows the displacement data and fitted curves for each analog individually.

The three C10 analogs retained highest affinity for GluK1 kainate receptor subunits relative to other kainate or AMPA receptor subunits, but their pharmacological profiles diverged in other ways (Fig. 2A–C and Table 1). The hydroxymethyl group in 10-HM-NDH reduced binding affinity to both GluK1 and GluK2 subunits by roughly an order of magnitude relative to the parent molecule NDH (K_i values 59 and 834 nM for GluK1 and GluK2, respectively; 95 % confidence interval [C.I.] 31 – 114 nM for GluK1 and 590 nM – 1.2 μM for GluK2, n = 3 – 5; Fig. 2A and Table 1). Surprisingly, this analog showed little appreciable binding affinity for GluK3 subunits at concentrations as high as 10 μM (Fig. 2A). Radioligand displacement by 10-HM-NDH was not significantly different from GluK5 (KA2) kainate receptor subunits or the GluA1 and GluA2 AMPA receptor subunits. No specific binding was obtained from GluK4-transfected membrane preparations, and therefore we were unable to determine analog affinities for this kainate receptor subunit.

The addition of a methyl group to 10-HM-NDH, to generate 10-MOM-NDH, resulted in a ~6-fold increase in binding affinity for GluK1 subunits (K_i of 10 nM; 95% C.I. of 5.9 – 18 nM, n = 3 – 5 experiments at each concentration, Fig. 2B), which was not significantly different from NDH itself (K_i of 7.7 nM) (Sanders et al., 2005). Unlike GluK1, however, binding to GluK2 was reduced by the extra methyl group, to a K_i of 2.4 μM (95% C.I.: 1.4 – 4.1 μM). Binding affinity for GluK3 remained very weak (K_i = 14.5 μM) with 10-HM-MOM-NDH.

Lastly, 8-desmethyl-10-HM-DH exhibited a K_i value of 7.2 nM for GluK1 subunits (95% C.I. of 4.3 – 12 nM, n = 3 – 5 experiments at each concentration; Fig. 2C), a 8-fold increase in affinity relative to 10-HM-NDH, from which it differs only in the C8 substituent (Fig. 1). Displacement of radioligand by 8-desmethyl-10-HM-DH from GluK2 subunits was similar to that of 10-HM-NDH (K_i value = 929 nM with 95% C.I. of 686 nM – 1.2 μM, n = 3–5). Strikingly, 8-desmethyl-10-HM-DH had a much higher affinity for GluK3 receptors (K_i = 397 nM; 95% C.I: 303 – 521 nM, n = 3 – 5) than did 10-HM-NDH. Thus, binding affinities of DH analogs for GluK3 receptors are highly sensitive to the molecular properties of the C8 functional group.

This hypothesis was tested further in radioligand displacement assays to measure the binding affinities of the parent molecules, DH and NDH, for GluK3 receptors, which had not been determined in previous studies (Fig. 3, Table 1). As well, we carried out a new set of displacement assays for NDH on GluK2 receptors, which had been performed previously (Sanders et al., 2005); for comparative purposes the figure also shows DH displacement of [^{3}H]kainate from GluK2 (Sakai et al., 2001b). We observed a clear divergence in affinity between DH and NDH for GluK3 that did not exist for GluK2 receptors. On GluK3 receptors, DH displaced radioligand with a K_i value of 5.4 nM (95% C.I. 3.8 – 7.8 nM), similar to its affinity for GluK2 (1.3 nM) (Sakai et al., 2001b). In contrast, NDH bound very weakly to GluK3 (K_i = 3.0 μM; 95% C.I.: 2.2 – 4.1 μM) relative to GluK2 (8.4 nM; 95% C.I.: 6.4 – 11.1 nM); the latter was somewhat higher affinity than was observed previously for NDH on GluK2 subunits (Sanders et al., 2005). The C8 hydroxyl group in NDH therefore reduces affinity for binding to all three primary kainate receptor subunits (GluK1–3) in comparison to the C8 methylamine in DH, and GluK3 is impacted most acutely by the nature of the functional group at C8, as evidenced by the ~1000-fold difference in affinity for the two ligands.

Pharmacological activity of C10 analogs on kainate receptors

DH and neoDH are both potent kainate receptor agonists, but a structurally related synthetic analog, 8,9-dideoxy-NDH (MSVIII-19), acts as a functional antagonist that effectively desensitizes receptors containing the GluK1 subunit (Frydenvang et al., 2009; Sakai et al., 2001b; Sanders et al., 2005). We therefore determined the pharmacological activity of the C10 analogs in whole-cell patch-clamp recordings. Saturating concentrations of glutamate (10 mM) were applied to transiently transfected HEK-293-T/17 cells, evoking control currents, before test applications of C10 analogs at relatively high concentrations (10–30 μM). Each of the three analogs elicited currents from GluK1-expressing cells (n = 3 – 5, Fig. 4A) and thus are agonists. 10-MOM-NDH (10 μM) was the most efficacious, producing current amplitudes ~25% of the control glutamate responses (Fig. 4A). 8-desmethyl-10-HM-DH (30 μM), in contrast, appeared to be a very weak agonist, gating only very modest currents from GluK1 receptors in a subset of recordings. Each of the three C10 analogs also elicited currents from GluK2-expressing cells (n = 3 – 5 recordings, Figure 4B); at the concentrations tested, 10-MOM-NDH was least efficacious on GluK2 receptors. Conversely, 8-desmethyl-10-HM-DH evoked currents larger in amplitude (relative to control glutamate-evoked currents) from GluK2 receptors compared to its actions on GluK1 receptors (Figure 4B). The analogs did not elicit current from GluK3-expressing cells (data not shown). Finally, 8-desmethyl-10-HM-DH (30 μM) evoked currents of very small amplitude (<10 pA) from GluK1/GluK4, GluK2/GluK4, GluK1/GluK5, and GluK2/GluK5 heteromeric receptors (n= 3 – 4 recordings for each receptor type, data not shown). In summary, these analogs are agonists for homomeric and heteromeric kainate receptors.

We previously demonstrated that DH and other high-affinity analogs induce a very stable, ligand-bound desensitized conformation of homomeric kainate receptors that occludes subsequent activation of the receptors for long periods of time (Lash et al., 2008; Sanders et al., 2005; Swanson et al., 2002). This prolonged desensitization can be assessed functionally by measuring the slow recovery of receptor currents evoked by a low-affinity agonist such as L-glutamate. Thus, to determine which C10 analogs similarly induce stable desensitization of homomeric kainate receptors, we measured the time course of recovery of glutamate-evoked currents after application of 10-HM-NDH, 10-MOM-NDH, and 8-desmethyl-10-HM-DH (each at 30 μM for 30 sec) to either GluK1 or GluK2 receptors (Fig. 5). Recovery of GluK3 receptors was also measured following application of 10-MOM-NDH and 8-desmethyl-10-HM-DH, which exhibited binding affinity for this receptor subunit. Amplitudes of glutamate-evoked currents following analog application were normalized to currents during the initial control period (before exposure to the C10 compounds). For those ligand-receptor

combinations that exhibited relatively slow recovery time courses, the data were fit to single or dual-exponential association functions to determine recovery time constants.

GluK1 receptors were most stably desensitized by the C10 analogs, consistent with the higher binding affinities relative to GluK2 or GluK3. 10-HM-NDH stabilized a desensitized state of GluK1 receptors that slowly recovered to a plateau amplitude of 70% of the control currents with a time constant of 2.4 ± 0.2 min (Fig. 5A). The plateau amplitudes were lower than controls because repeated glutamate application to GluK1 caused a progressive reduction (run-down) of the currents independent of 10-HM-NDH application to the receptor (Lash et al., 2008). In contrast, 10-HM-NDH did not cause prolonged desensitization of GluK2 receptors, which recovered within less than a minute. (The precise time course is difficult to measure because glutamate is applied at 20 seconds intervals to avoid inducing further desensitization.)

After exposure to 10-MOM-NDH, the glutamate-evoked current from GluK1 receptors recovered more slowly (τ_{rec} of 6.7 ± 0.4 min) and was attenuated to a greater degree than observed with 10-HM-NDH (Fig. 5B). The plateau amplitude was 45% of control amplitudes, smaller than that accounted for by run-down of glutamate-evoked currents. 10-MOM-NDH therefore induces a stable desensitized state similar to those observed with the natural toxins DH and NDH (Sanders et al., 2005;Swanson et al., 2002) and other synthetic analogs (Lash et al., 2008). As with 10-HM-DH, desensitization of GluK2 receptors in response to 10-MOM-NDH was relatively brief and reversible, and GluK3 receptors responded in a similar fashion (Fig. 5B).

Responses to 8-desmethyl-10-HM-DH were very similar to that of 10-HM-NDH. This compound also desensitized GluK1 receptors for prolonged times after application, yielding a time constant of 2.5 ± 0.5 min (Fig. 5C), but receptors recovered to a plateau level at which currents were 69% of the control amplitude. On the other hand, both GluK2 and GluK3, as well as heteromeric receptors containing the GluK4 or GluK5 subunits, rapidly recovered within a minute to control amplitudes (Fig. 5C and data not shown). In these particular recordings, we noted that the run-down of GluK3 currents during the control period was substantial, which might account for the reduced plateau level observed for the averaged GluK3 responses following 8-desmethyl-10-HM-DH.

Molecular interactions underlying the pharmacological specificity of the C8 functional group for kainate receptor subunits

The binding affinity for ligands containing a C8 hydroxyl group (e.g., NDH, 10-HM-NDH) was much lower on GluK3 compared to GluK2 receptors; this subunit-specific difference was not present to the same magnitude for C8 methylamine- or amine-containing ligands (e.g., DH, 8-desmethyl-DH). Variability in the direct or indirect interactions between ligands and receptor protein within the binding pocket could give rise to disparity in the apparent binding affinities we measured experimentally. Comparison of GluK1–3 primary sequences in the space occupied by the 8-aminomethyl group of DH in the GluK1-DH crystal structure (Frydenvang et al., 2009) suggested that the difference in affinity for DH *versus* NDH, and 8-desmethyl-10-HM-DH *versus* 10-HM-NDH, arises from the amino acid at position 444 (GluK1 numbering). This is a tyrosine in GluK1 and GluK2 but a phenylalanine in GluK3 subunits. To explore this possibility, we performed MD simulations of NDH complexed with either GluK2 or GluK3 LBCs using the crystal structure of DH and GluK1 as the template for homology models (Frydenvang et al., 2009).

We first simulated the interactions between docked 8-desmethyl-10-HM-DH ligand with the GluK1-, GluK2-, and GluK3-LBCs (Fig. 6, with amino acids identified according to their position in the full-length subunits). In GluK1 and GluK2, the side-chain hydroxyl group of Ser/Thr741 is oriented towards Tyr444 (Tyr443 in GluK2) and forms a hydrogen bond with

the C8 amine (Fig. 6), as was observed in the crystal structure of the GluK1-DH complex (Frydenvang et al., 2009). In GluK3, however, the absence of the polar group in Phe446, the analogous residue, induces a rotation by Thr742 such that hydrophobic packing occurs between its side chain methyl group and the aromatic ring of Phe446 (Fig. 6, at the site of the arrow). This in turn results in donation of an additional hydrogen bond by the hydroxyl group in Thr742 to the main chain carbonyl oxygen atom of Glu739 in GluK3. This subtle shift in the hydrogen bonding network is predicted to impact the binding configuration of the C8 substituent in two critical ways to account for the subunit specificity of the ligands: (1) amine groups in DH and 8-desmethyl-10-HM-DH interact favorably with both GluK2 and GluK3 because of the favorable hydrogen bonding to both the γ-carboxylate groups of Glu738/739 and the side chain hydroxyl of Ser741/Thr742, whereas the (2) hydroxyl groups in NDH and 10-HM-NDH are forced into an unfavorable interaction with the negatively charged acceptor oxygen atoms at the same two sites. Although the side chain hydroxyls of Ser/Thr741 in GluK1 and GluK2 could donate a hydrogen bond to the oxygen of an 8-hydroxyl group in the ligand, the intramolecular hydrogen bond network of the receptor would nevertheless be disturbed, increasing the intramolecular energy and lowering binding affinity. Accordingly, the ligands with an 8-amino(methyl) group have higher binding affinities than 8-hydroxyl group ligands for all three receptors, but most notably for GluK3 subunits (Table 1).

We tested these predictions in two ways. First, we generated reciprocal mutants at the Tyr443/Phe446 residues in GluK2 and GluK3 subunits, respectively. Second, we attempted to alleviate the repulsion between C8-hydroxyl groups and oxygens contributed by residues in the GluK3 receptor though mutation of Thr520 in GluK3 to an alanine contained at the analogous site in GluK2 (Ala518) (Fig. 6, site indicated by the grey arrowhead). Thr520 forms a hydrogen bond with Glu739; mutation to an alanine eliminates this interaction and is predicted to shift the position of the γ-carboxylate of Glu739, which donates the other of the two oxygens that negatively impacts binding of C8-hydroxyl ligands (NDH, 8-desmethyl-10-HM-DH) in the presence of Phe446.

NDH exhibits the most marked difference in affinity for GluK2 *versus* GluK3, and thus we compared the impact of reciprocal mutations to the two receptor sites on binding affinity for this particular ligand. Saturation binding isotherms with the single mutants GluK2(Y443F), GluK2(A518T), GluK3(F446Y), GluK3(T520A), as well as the double mutants GluK2(Y443F/A518T) and GluK3(Y446F/T520A), verified that the mutations did not significantly alter the affinity for [^{3}H]kainate of these receptors (see Methods). In radioligand displacement assays to determine the K_i values for NDH, we found that each of the single-site mutants in GluK2 subunits resulted in decreased affinity (Fig. 7A). GluK2(Y443F) nearly reproduced the affinity for NDH on GluK3, reducing affinity by 100-fold, to a K_i of 895 nM, whereas GluK2(A518T) more modestly decreased the affinity for NDH by ~7-fold to 61 nM (compared to 8.5 nM for GluK2 receptors; n=3–5). In contrast, single-site mutations of the GluK3 subunit had little effect on the affinity for NDH (Fig. 7B); K_i values were 547 nM and 1.4 μM for GluK3(F446Y) and GluK3(T520A), respectively (n = 3–5).

These results suggested to us that the hydrogen bond network critical for stabilization of NDH binding to the receptor was readily disrupted by imposition of a single unfavorable interaction. We next tested if reciprocal mutation of both sites in GluK2 and GluK3 generated binding configurations analogous to the complementary wildtype receptors. GluK2(Y443F/A518T) receptors exhibited binding affinities similar to that of GluK3 receptors (K_i = 972 nM for the double mutant, n = 3–5, Fig. 7C), as was expected based on the impact of the single mutation from tyrosine to phenylalanine at residue 443/446. Conversely, GluK3(F446Y/T520A) receptors exhibited a modest but significant 10-fold increase in their binding affinity for NDH (K_i of 260 nM, n = 3–5, Fig. 7C). Thus, reciprocal mutation of the two sites did not reconstitute the high-affinity interaction between NDH and GluK2 subunits, but did enhance the binding

to a significant degree. These results largely are consistent with the prediction of the MD simulations, particularly with respect to the importance of the Tyr443/Phe446 variation, but clearly other determinants exist in the ligand-binding pocket that shape the hydrogen bond network formed by ligands containing a C8 hydroxyl group.

Molecular interactions underlying the pharmacological specificity of the C10 functional group for kainate receptor subunits

MD simulations also were performed to explore the molecular basis for the selectivity of C10-substituted ligand for the GluK1 subunit. As shown in Table 1, addition of the 10-hydroxymethyl group reduced affinity for GluK1 by ~8-fold when compared to its parent molecule NDH. The 10-hydroxymethyl group is predicted to occupy a hydrophobic niche in the ligand binding pocket of GluK1 formed by the side chains of Ser721, Leu541, Ile725, Leu735, Met737, and Val745 (shown with transparent surfaces in Figure 8A). The position of Ile725 is stabilized further by hydrophobic packing of Leu729 and Leu752 (not shown). Binding into this niche is impacted unfavorably in GluK2 and GluK3 by bulkier amino acids at positions 721/722 (GluK2/GluK3: asparagine) and 735 (GluK2: phenylalanine) that project into the space available for the C10 hydroxymethyl group, as well as the more restricted rotamer conformations available to Asn721, resulting in the substantial reduction in affinity for GluK2. Analogous interactions likely underlie the pharmacological activity of 8-desmethyl-10-HM-DH, which contains an equivalent C10 functional group. The methoxymethyl group in 10-MOM-NDH, which binds more favorably than 10-HM-NDH to GluK1 and is a more efficacious agonist at concentrations we tested, locks itself into the hydrophobic pocket more optimally because of the greater hydrophobicity conferred by the additional methyl group. The added bulk at the C10 position proves a liability, however, in the presence of the steric hindrance introduced by the larger 721 and 735 residues in GluK2, resulting in ~290-fold weaker binding affinity when compared to NDH (Table 1). In summary, these analogs are selective for GluK1 subunits because the C10 functional groups on the ligands access the comparatively larger hydrophobic niche within the binding pocket of kainate receptor subunits (Mayer, 2005;Pentikäinen et al., 2003).

DISCUSSION

Kainate receptors are thought to serve modulatory roles in the mammalian CNS, maintaining a balance between excitation and inhibition through activities at both pre- and postsynaptic sites. The potential efficacy of targeting these receptors in treatment of neurological diseases is still largely unknown but is an area of active clinical exploration (Jane et al., 2008; Swanson, 2009). Preclinical data is promising; antagonists selective for GluK1-containing receptors show efficacy in models of a number of pathologies, including migraine (Filla et al., 2002), pain (Dominguez et al., 2005; Jones et al., 2006), anxiety (Alt et al., 2006; Alt et al., 2007), and epilepsy (Smolders et al., 2002). Antagonists with equivalent levels of selectivity for other kainate receptors, containing GluK2 or GluK3 as the principle subunit, have not yet been isolated and characterized, and thus the therapeutic potential derived from selective inhibition of these receptors remains speculative.

Our ongoing characterization of structural analogs of the marine-derived natural toxins DH and NDH aims to identify ligands with novel specificity for kainate receptors and to understand the structural components important for conferring selectivity and activity at these receptors (Lash et al., 2008; Sanders et al., 2005; Sanders et al., 2006). These molecules have been modified extensively for the purpose of generating novel ligands and activities (reviewed in Swanson and Sakai, 2009). We found previously that the C8 and C9 position, in particular, confer affinity and selectivity for the kainate receptor subunits GluK1–3 (Lash et al., 2008; Postila et al., 2009). Removal of both functional groups at these positions, in 8,9-dideoxy-NDH

(or MSVIII-19), produced an extraordinarily weak partial agonist with potent desensitizing properties suitable for use as an effective GluK1 receptor antagonist (Frydenvang et al., 2009; Sanders et al., 2005). In the current study, we focused on a novel trio of DH/NDH analogs with functional additions at the C10 position (Sasaki et al., 2006). Our principle observation was that the C10 analogs remained high-affinity agonists for the GluK1 but not other kainate receptors, and that this GluK1 selectivity was attributable to the presence of a hydrophobic pocket readily accessed by bulky C10 functional groups. As an ancillary and unexpected observation, we found that one of the parent natural toxins, NDH, markedly differed in its affinity for GluK2 and GluK3 subunits. This subunit selectivity suggests that it may be possible to generate ligands selective for kainate receptor subunits, in addition to those that exist for GluK1 receptors, despite the steric restrictions imposed by smaller binding pockets in GluK2 and GluK3 (Mayer, 2005; Pentikäinen et al., 2003).

As with the C10 compounds examined here, most DH analogs bind with highest affinity to the GluK1 subunit. This selectivity is not unique to DH-related molecules; a generally similar pattern of specificity exists for synthetic analogs derived from willardiine (Dolman et al., 2007; Dolman et al., 2006; Dolman et al., 2005; More et al., 2004), a natural product isolated from *Acacia* seeds. The LBD of GluK1 is physically larger than other kainate or AMPA receptor subunits, which may in part underlie the predominance of ligands that bind to this subunit relative to GluK2 or GluK3 (Mayer, 2005; Mayer et al., 2006; Pentikäinen et al., 2003). Based on our MD simulations, C10 functional groups access one of the expanded pockets within the GluK1 LBD that is constrained sterically in GluK2 and GluK3; most notably, the addition of a bulky hydrophobic methoxymethyl group in 10-MOM-NDH has only a minor impact on its activity on GluK1 receptors but reduces binding to GluK2 by ~100-fold (while remaining an agonist). The several-fold lower affinity of 10-HM-NDH relative to its larger, more hydrophobic analog 10-MOM-NDH also demonstrates that reactive polar group creates unfavorable conformations within this small sub-domain of the GluK1 binding pocket.

MD simulations also revealed the strikingly subtle rearrangements in the ligand-receptor hydrogen bonding network that likely underlie the divergence in C8 amine- *versus* hydroxyl-substituted analog affinities for GluK2 and GluK3. Those analogs containing an amine group at this position (DH and 8-desmethyl-10-HM-DH) bind with equivalent affinity to both GluK2 and GluK3 or exhibit a several-fold preference for the latter subunit, respectively. In contrast, C8 hydroxyl analogs (NDH and 10-HM-NDH) bind to GluK2 but not to GluK3 with any significant degree of affinity. The simulations suggested that variation at Tyr443/Phe446 (in GluK2 and GluK3, respectively) in part constituted an important molecular determinant predicted to underlie this divergence in binding affinity, but not because it formed a direct hydrogen bond with the C8 functional group of the ligand. Instead, the Tyr-Phe difference affected configurations of the receptor side-chain residues, creating more (GluK2) or less (GluK3) favorable orientations of electron donor groups in Glu738/739 and Ser741/Thr742. This supposition was supported by the mutagenic studies that aimed to alter the relevant hydrogen bond network through exchange of Tyr443/Phe446 or alter the positioning of the γ-carboxyl group in Glu738/739 by exchanging Ala518 and Thr520. It was clear from these studies that disruption of binding affinity for NDH was straightforward to achieve in GluK2 with single unfavorable mutations. On the other hand, simply introducing two reciprocal mutations into GluK3 did not recapitulate the higher affinity and, presumably, the more favorable binding configuration in GluK2. Future experiments will be required to resolve additional determinants that confer the optimal binding environment for the ligands.

We noted previously that the binding affinity of DH analogs for recombinant GluK1 subunits was strongly correlated with their convulsant potency in mice, suggesting that receptors containing GluK1 underlie agonist-induced seizures (Lash et al., 2008). Comparison of the pharmacological properties of the C10 analogs with preliminary *in vivo* convulsant data support

a central role for GluK1, consistent with the previous data, but also suggest that other kainate receptor subunits contribute to seizure phenotypes. That is, 8-desmethyl-10-HM-DH had the highest GluK1 affinity in our assays but was significantly less potent than 10-HM-NDH in eliciting seizures following i.c.v. injection (1.3 nmol/mouse *versus* 0.11 nmol/mouse, respectively; (R. Sakai, unpublished data and Sasaki et al., 2006). Pharmacological and behavioral analysis of a larger set of DH-based analogs will be required to more clearly define the complex relationships between receptor subunit affinity (and efficacy) and seizurogenic potencies. Evidence exists that both GluK1- and GluK2-containing receptors play roles in generating synchronized firing. For example, GluK1 antagonists are potent anticonvulsants in both *in vitro* and *in vivo* models of epilepsy (Smolders et al., 2002) and chronic epileptic rats (Epsztein et al., 2005). As well, GluK2-containing receptors have been associated with convulsant activity; these receptors are predominant in hippocampal loci of epileptogenesis (Ben-Ari, 1985; Egebjerg et al., 1991) and in part underlie kainate-induced seizurogenesis in animals (Mulle et al., 1998). The anticonvulsant potential of GluK2 antagonists is entirely unknown, however, because selective compounds have not been isolated and characterized to date. Synthetic modification of existing template molecules, such as DH and willardiine, has led to key insights into the molecular basis for ligand activity and specificity, and additional modification may yet expand the complement of useful antagonists to encompass those kainate receptor subunits that remain elusive pharmacological targets.

Acknowledgments

This study was supported by the National Graduate School in Informational and Structural Biology (PP), the Sigrid Jusélius Foundation (OTP), Grant-in Aid for Scientific Research awards from the Japanese Ministry of Education, Culture, Sports, Science and Technology (Nos. 16073202 and 17380125 to MaS and RS, respectively), and the National Institute for Neurological Diseases and Stroke (R01 NS44322 to GTS). The Finnish IT Center for Science (Espoo, Finland), is acknowledged for access to the computational resources used for MD simulations (project JYY2516 to OTP).

REFERENCES

Alt A, Weiss B, Ogden AM, Li X, Gleason SD, Calligaro DO, Bleakman D, Witkin JM. In vitro and in vivo studies in rats with LY293558 suggest AMPA/kainate receptor blockade as a novel potential mechanism for the therapeutic treatment of anxiety disorders. Psychopharmacology (Berl) 2006;185:240–247. [PubMed: 16470401]

Alt A, Weiss B, Ornstein PL, Gleason SD, Bleakman D, Stratford RE Jr, Witkin JM. Anxiolytic-like effects through a GLU(K5) kainate receptor mechanism. Neuropharmacology 2007;52:1482–1487. [PubMed: 17418283]

Bayly C, Cieplak P, Cornell W, Kollman P. A well-behaved electrostatic potential based method using charge restraints for deriving atomic charges: the RESP model. J. Phys. Chem 1993;97:10269–10280.

Ben-Ari Y. Limbic seizure and brain damage produced by kainic acid: mechanisms and relevance to human temporal lobe epilepsy. Neuroscience 1985;14:375–403. [PubMed: 2859548]

Cieplak P, Cornell W, Bayly C, Kollman P. Application of the multimolecule and multiconformational RESP methodology to biopolymers-charge derivation for DNA, RNA, and proteins. J. Comput. Chem 1995;16:1357–1377.

Cornell W, Cieplak P, Bayly C, Kollman P. Application of the RESP Charges to Calculate Conformational Energies, Hydrogen Bond Energies, and Free Energies of Solvation. J. Am. Chem. Soc 1993;115:9620–9631.

Darden T, York Y, Pedersen L. Particle mesh Ewald: An W log(N) method for Ewald sums in large systems. J. Chem. Phys 1993;98:10089–10092.

Dolman NP, More JC, Alt A, Knauss JL, Pentikainen OT, Glasser CR, Bleakman D, Mayer ML, Collingridge GL, Jane DE. Synthesis and pharmacological characterization of N3-substituted willardiine derivatives: role of the substituent at the 5-position of the uracil ring in the development of highly potent and selective GLUK5 kainate receptor antagonists. J. Med. Chem 2007;50:1558–1570. [PubMed: 17348638]

Dolman NP, More JC, Alt A, Knauss JL, Troop HM, Bleakman D, Collingridge GL, Jane DE. Structure-activity relationship studies on N3-substituted willardiine derivatives acting as AMPA or kainate receptor antagonists. J. Med. Chem 2006;49:2579–2592. [PubMed: 16610801]

Dolman NP, Troop HM, More JC, Alt A, Knauss JL, Nistico R, Jack S, Morley RM, Bortolotto ZA, Roberts PJ, Bleakman D, Collingridge GL, Jane DE. Synthesis and pharmacology of willardiine derivatives acting as antagonists of kainate receptors. J. Med. Chem 2005;48:7867–7881. [PubMed: 16302825]

Dominguez E, Iyengar S, Shannon HE, Bleakman D, Alt A, Arnold BM, Bell MG, Bleisch TJ, Buckmaster JL, Castano AM, Del Prado M, Escribano A, Filla SA, Ho KH, Hudziak KJ, Jones CK, Martinez-Perez JA, Mateo A, Mathes BM, Mattiuz EL, Ogden AM, Simmons RM, Stack DR, Stratford RE, Winter MA, Wu Z, Ornstein PL. Two prodrugs of potent and selective GluR5 kainate receptor antagonists actives in three animal models of pain. J. Med. Chem 2005;48:4200–4203. [PubMed: 15974569]

Egebjerg J, Bettler B, Hermans-Borgmeyer I, Heinemann S. Cloning of a cDNA for a glutamate receptor subunit activated by kainate but not AMPA. Nature 1991;351:745–748. [PubMed: 1648177]

Epsztein J, Represa A, Jorquera I, Ben-Ari Y, Crepel V. Recurrent mossy fibers establish aberrant kainate receptor-operated synapses on granule cells from epileptic rats. J. Neurosci 2005;25:8229–8239. [PubMed: 16148230]

Filla SA, Winter MA, Johnson KW, Bleakman D, Bell MG, Bleisch TJ, Castano AM, Clemens-Smith A, del Prado M, Dieckman DK, Dominguez E, Escribano A, Ho KH, Hudziak KJ, Katofiasc MA, Martinez-Perez JA, Mateo A, Mathes BM, Mattiuz EL, Ogden AM, Phebus LA, Stack DR, Stratford RE, Ornstein PL. Ethyl (3S,4aR,6S,8aR)-6-(4-ethoxycar- bonylimidazol-1-ylmethyl)decahydroiso-quinoline-3-carboxylic ester: a prodrug of a GluR5 kainate receptor antagonist active in two animal models of acute migraine. J. Med. Chem 2002;45:4383–4386. [PubMed: 12238915]

Frydenvang K, Lash LL, Naur P, Postila PA, Pickering DS, Smith CM, Gajhede M, Sasaki M, Sakai R, Pentikäinen OT, Swanson GT, Kastrup JS. Full domain closure of the ligand-binding core of the ionotropic glutamate receptor iGluR5 induced by the high-affinity agonist dysiherbaine and the functional antagonist MSVIII-19. J. Biol. Chem 2009;284:14219–14229. [PubMed: 19297335]

Jane DE, Lodge D, Collingridge GL. Kainate receptors: Pharmacology, function and therapeutic potential. Neuropharmacology 2008;56:90–113. [PubMed: 18793656]

Jones CK, Alt A, Ogden AM, Bleakman D, Simmons RM, Iyengar S, Dominguez E, Ornstein P, Shannon HE. Anti-allodynic and anti-hyperalgesic effects of selective competitive GLUK5 (GluR5) ionotropic glutamate receptor antagonists in the capsaicin and carrageenan models in rats. J. Pharmacol. Exp. Ther 2006;319:396–404. [PubMed: 16837561]

Jones G, Willett P, Glen RC. Molecular recognition of receptor sites using a genetic algorithm with a description of desolvation. J. Mol. Biol 1995;245:43–53. [PubMed: 7823319]

Jones G, Willett P, Glen RC, Leach AR, Taylor R. Development and validation of a genetic algorithm for flexible docking. J. Mol. Biol 1997;267:727–748. [PubMed: 9126849]

Lash LL, Sanders JM, Akiyama N, Shoji M, Postila P, Pentikainen OT, Sasaki M, Sakai R, Swanson GT. Novel analogs and stereoisomers of the marine toxin neodysiherbaine with specificity for kainate receptors. J. Pharmacol. Exp. Ther 2008;324:484–496. [PubMed: 18032572]

Lehtonen JV, Still DJ, Rantanen VV, Ekholm J, Bjorklund D, Iftikhar Z, Huhtala M, Repo S, Jussila A, Jaakkola J, Pentikäinen O, Nyronen T, Salminen T, Gyllenberg M, Johnson MS. BODIL: a molecular modeling environment for structure-function analysis and drug design. J. Comput. Aided Mol. Des 2004;18:401–419. [PubMed: 15663001]

Lovell SC, Word JM, Richardson JS, Richardson DC. The penultimate rotamer library. Proteins 2000;40:389–408. [PubMed: 10861930]

Mayer ML. Crystal structures of the GluR5 and GluR6 ligand binding cores: molecular mechanisms underlying kainate receptor selectivity. Neuron 2005;45:539–552. [PubMed: 15721240]

Mayer ML, Ghosal A, Dolman NP, Jane DE. Crystal structures of the kainate receptor GluR5 ligand binding core dimer with novel GluR5-selective antagonists. J Neurosci 2006;26:2852–2861. [PubMed: 16540562]

More JC, Nistico R, Dolman NP, Clarke VR, Alt AJ, Ogden AM, Buelens FP, Troop HM, Kelland EE, Pilato F, Bleakman D, Bortolotto ZA, Collingridge GL, Jane DE. Characterisation of UBP296: a

novel, potent and selective kainate receptor antagonist. Neuropharmacology 2004;47:46–64. [PubMed: 15165833]

Mulle C, Sailer A, Pérez-Otaño I, Dickinson-Anson H, Castillo PE, Bureau I, Maron C, Gage FH, Mann JR, Bettler B, Heinemann SF. Altered synaptic physiology and reduced susceptibility to kainate-induced seizures in GluR6-deficient mice. Nature 1998;392:601–605. [PubMed: 9580260]

Naur P, Vestergaard B, Skov LK, Egebjerg J, Gajhede M, Kastrup JS. Crystal structure of the kainate receptor GluR5 ligand-binding core in complex with (*S*)-glutamate. FEBS Lett 2005;579:1154–1160. [PubMed: 15710405]

Pentikäinen OT, Settimo L, Keinänen K, Johnson MS. Selective agonist binding of (S)-2-amino-3-(3-hydroxy-5-methyl-4-isoxazolyl)propionic acid (AMPA) and 2S-(2alpha,3beta,4beta)-2-carboxy-4-(1-methylethenyl)-3-pyrrolidineacetic acid (kainate) receptors: a molecular modeling study. Biochem. Pharmacol 2003;66:2413–2425. [PubMed: 14637199]

Phillips JC, Braun R, Wang W, Gumbart J, Tajkhorshid E, Villa E, Chipot C, Skeel RD, Kale L, Schulten K. Scalable molecular dynamics with NAMD. J. Comp. Chem 2005;26:1781–1802. [PubMed: 16222654]

Postila PA, Swanson GT, Pentikainen OT. Exploring kainate receptor pharmacology using molecular dynamics simulations. Neuropharmacology. 2009

Puranam RS, Eubanks JH, Heinemann SF, McNamara JO. Chromosomal localization of gene for human glutamate receptor subunit-7. Som. Cell Mol. Gen 1993;19:581–588.

Sakai R, Kamiya H, Murata M, Shimamoto K. Dysiherbaine: a new neurotoxic amino acid from the Micronesian marine sponge *Dysidea herbacea*. J. Am. Chem. Soc 1997;119:4112–4116.

Sakai R, Koike T, Sasaki M, Shimamoto K, Oiwa C, Yano A, Suzuki K, Tachibana K, Kamiya H. Isolation, structure determination, and synthesis of neodysiherbaine A, a new excitatory amino acid from a marine sponge. Org. Lett 2001a;3:1479–1482. [PubMed: 11388846]

Sakai R, Swanson GT, Shimamoto K, Green T, Contractor A, Ghetti A, Tamura-Horikawa Y, Oiwa C, Kamiya H. Pharmacological properties of the potent epileptogenic amino acid dysiherbaine, a novel glutamate receptor agonist isolated from the marine sponge *Dysidea herbacea*. J. Pharmacol. Exp. Ther 2001b;296:650–658. [PubMed: 11160654]

Sanders JM, Ito K, Settimo L, Pentikäinen OT, Shoji M, Sasaki M, Johnson MS, Sakai R, Swanson GT. Divergent pharmacological activity of novel marine-derived excitatory amino acids on glutamate receptors. J. Pharmacol. Exp. Ther 2005;314:1068–1078. [PubMed: 15914675]

Sanders JM, Pentikäinen OT, Settimo L, Pentikainen U, Shoji M, Sasaki M, Sakai R, Johnson MS, Swanson GT. Determination of binding site residues responsible for the subunit selectivity of novel marine-derived compounds on kainate receptors. Mol. Pharmacol 2006;69:1849–1860. [PubMed: 16537793]

Sasaki M, Tsubone K, Shoji M, Oikawa M, Shimamoto K, Sakai R. Design, total synthesis, and biological evaluation of neodysiherbaine A derivative as potential probes. Bioorg. Med. Chem. Lett 2006;16:5784–5787. [PubMed: 16949819]

Schlick T, Skeel RD, Brunger AT, Kalé LV, Board JAJ, Hermans J, Schulteny K. Algorithmic Challenges in Computational Molecular Biophysics. J. Comp. Physics 1999;151:9–48.

Smolders I, Bortolotto ZA, Clarke VR, Warre R, Khan GM, O'Neill MJ, Ornstein PL, Bleakman D, Ogden A, Weiss B, Stables JP, Ho KH, Ebinger G, Collingridge GL, Lodge D, Michotte Y. Antagonists of GLU_{K5}-containing kainate receptors prevent pilocarpine-induced limbic seizures. Nat. Neurosci 2002;5:796–804. [PubMed: 12080343]

Swanson GT. Targeting AMPA and kainate receptors in neurological disease: therapies on the horizon? Neuropsychopharmacology 2009;34:249–250. [PubMed: 19079074]

Swanson GT, Green T, Sakai R, Contractor A, Che W, Kamiya H, Heinemann SF. Differential activation of individual subunits in heteromeric kainate receptors. Neuron 2002;34:589–598. [PubMed: 12062042]

Swanson GT, Sakai R. Ligands for ionotropic glutamate receptors. Prog. Mol. Subcell. Biol 2009;46:123–157. [PubMed: 19184587]

Toukmaji A, Sagui C, Board J, Darden T. Efficient particle-mesh Ewald based approach to fixed and induced dipolar interactions. J. Chem. Phys 2000;113:10913–10927.

Wang J, Wang W, Kollman PA, Case DA. Automatic atom type and bond type perception in molecular mechanical calculations. J. Mol. Graph. Model 2006;25:247–260. [PubMed: 16458552]

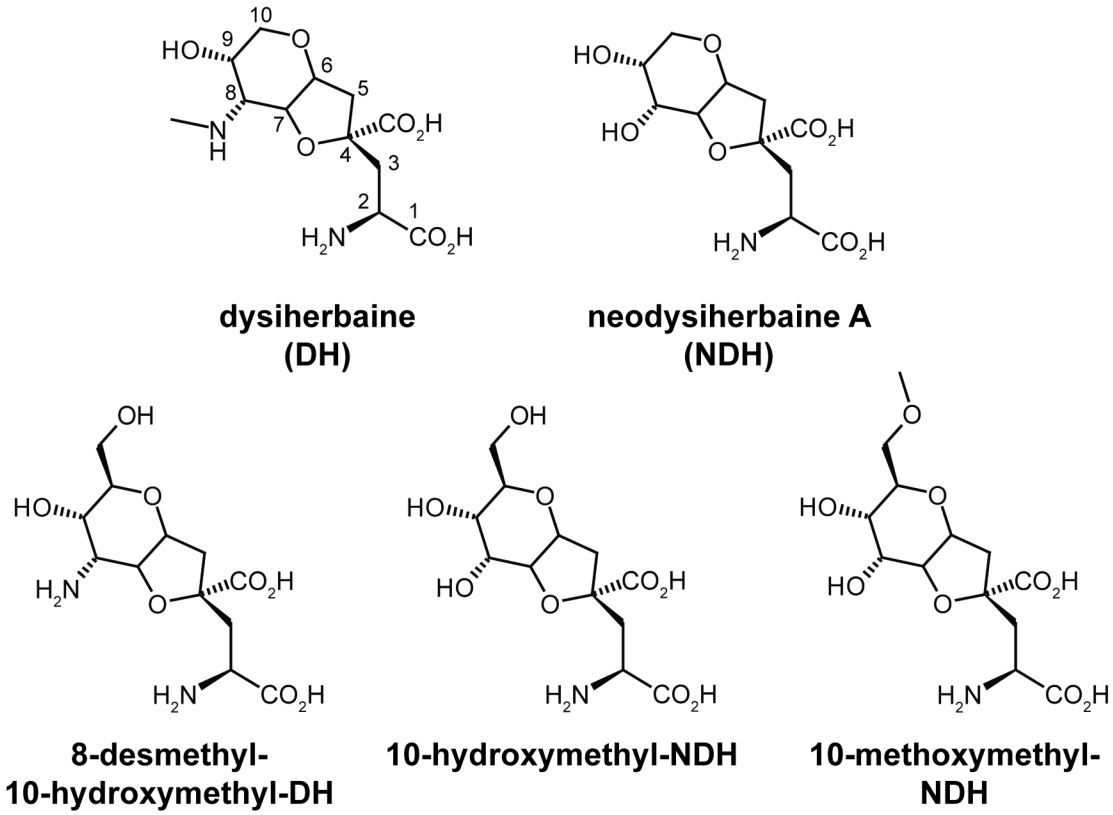

Figure 1.
Two dimensional structures of the synthetic C10 analogs of DH. The parent marine toxins, dysiherbaine (DH) and neodysiherbaine (NDH) are shown in the top row of structures. Numbering of the carbons is shown for the DH structure.

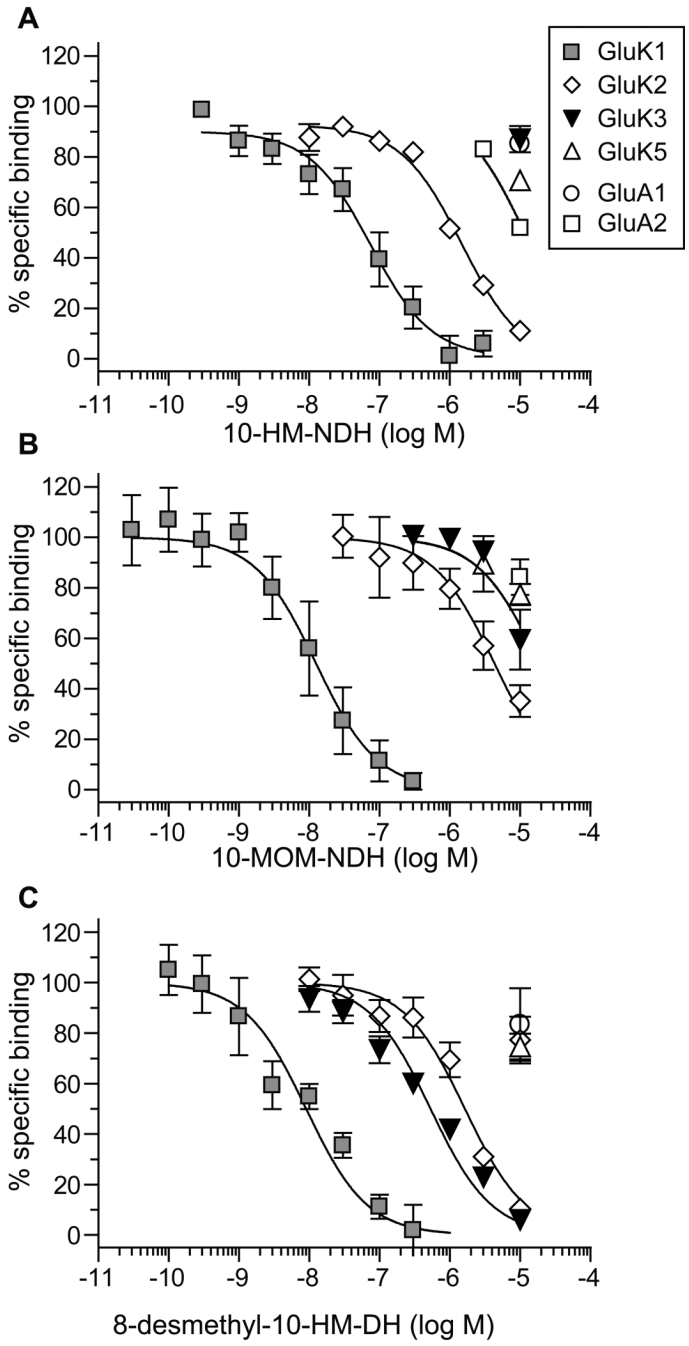

Figure 2.

C10 analogs of DH bind with highest affinity to GluK1 subunits in radioligand displacement assays. Displacement of [^{3}H]kainate or [^{3}H]AMPA from kainate and AMPA receptor subunits, respectively, for (**A**) 10-HM-NDH, (**B**) 10-MOM-NDH, and (**C**) 8-desmethyl-10-HM-DH. Symbols representing data from GluK1–3, GluK5, and GluA1–2 subunits are as shown in the boxed key in **A**. Data was fit with a one-site competition curve with fixed minima (0%) and maxima (100%) (n = 3–5 for each concentration of analog on each receptor subunit). K_i values derived from this data are given in Table 1.

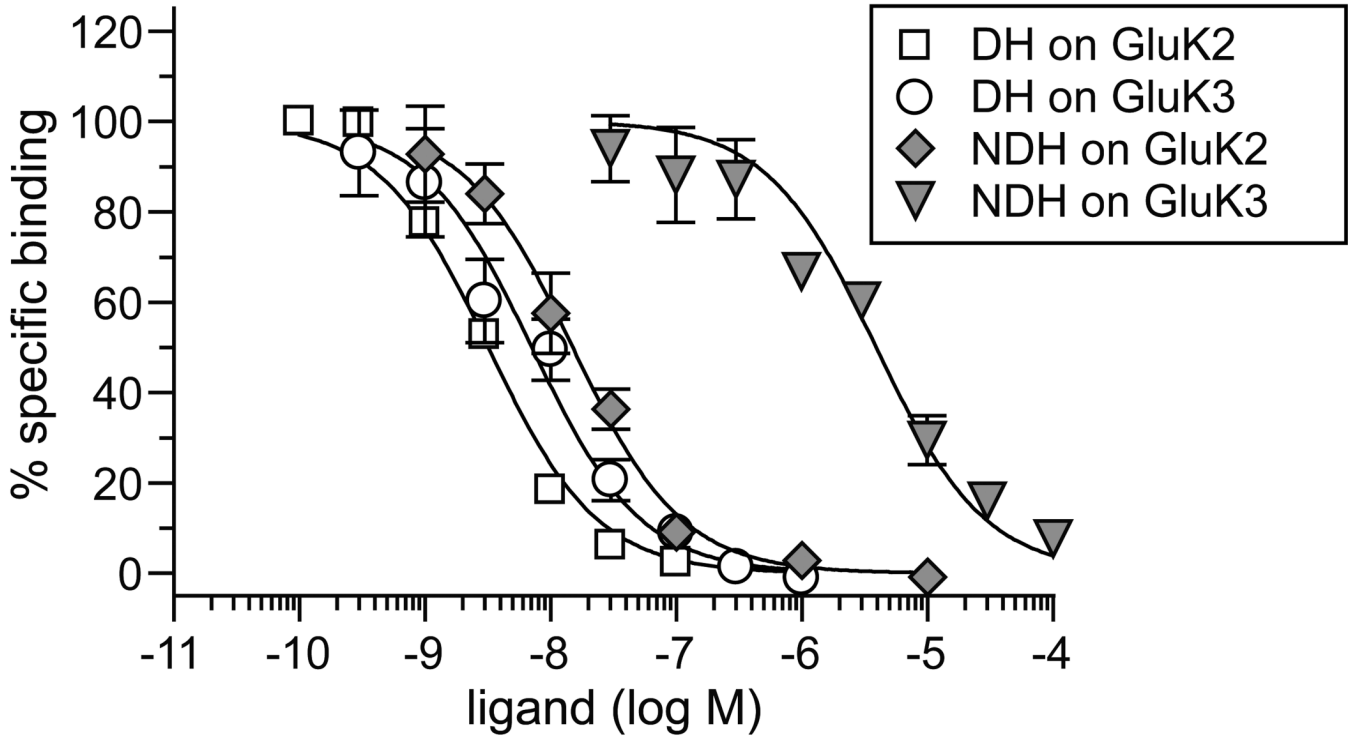

Figure 3.

NDH, but not DH, shows ~100-fold selectivity for GluK2 over GluK3 subunits. Displacement of [^{3}H]kainate from GluK2 and GluK3 subunits by DH and NDH. The competition curve for DH on GluK2 is from previously published data and is shown only for the sake of comparison (Sakai et al., 2001b). Data was fit with a one-site competition curve with fixed minima (0%) and maxima (100%) (n = 3–5 for each concentration of analog on each receptor subunit). K_i values derived from this data are given in Table 1.

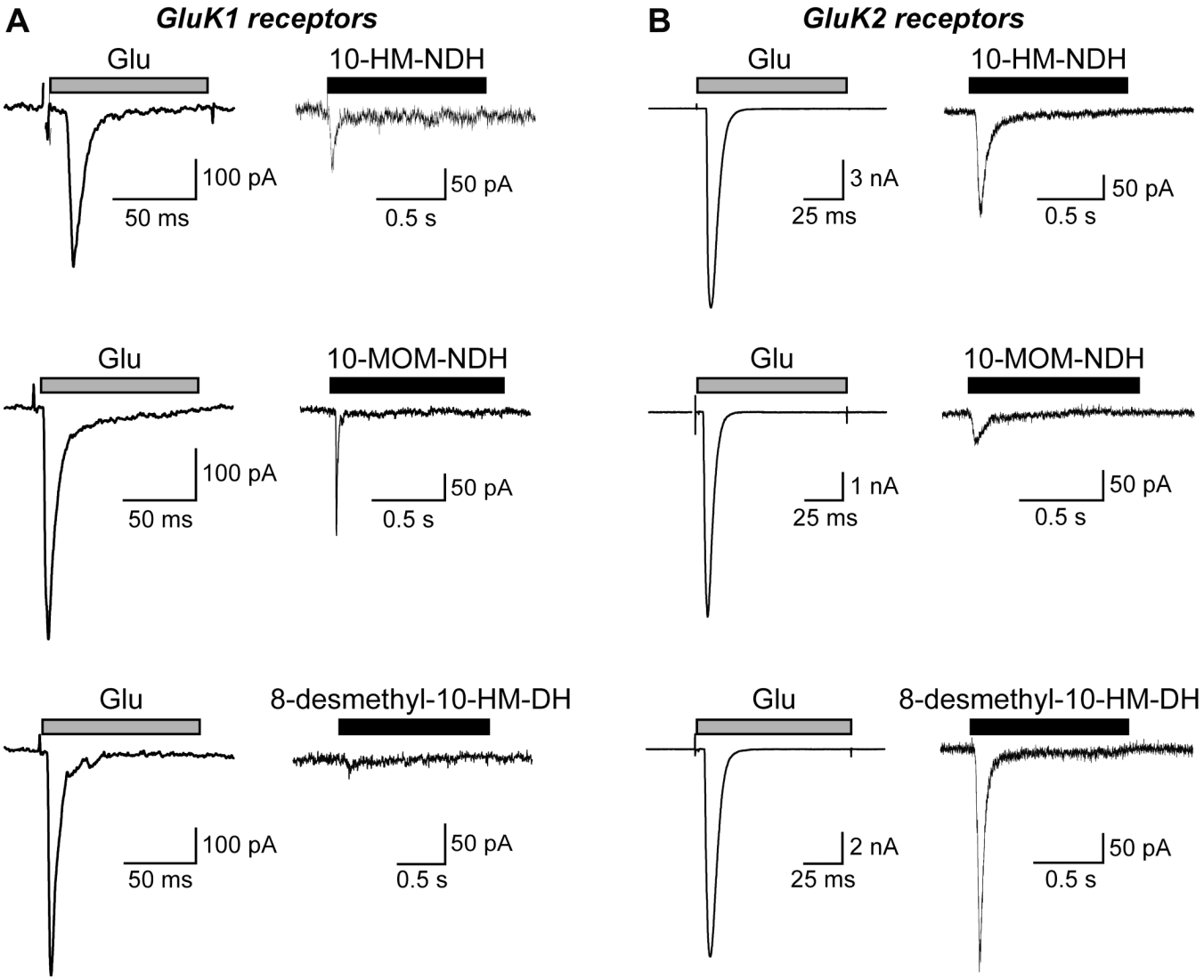

Figure 4.

The C10 analogs of DH are kainate receptor agonists. (**A**). Representative GluK1 receptor whole-cell currents evoked by application of glutamate (10 mM, 100 ms) or the C10 analogs (30 μM, 1 sec). (**B**). Representative currents from GluK2 receptors with the same set of agonists. Cells were held at −70 mV, lifted from the coverslip into a laminar solution stream, and agonists were fast-applied with a piezoceramic translation system. Traces are representative of at least 3 recordings under each condition.

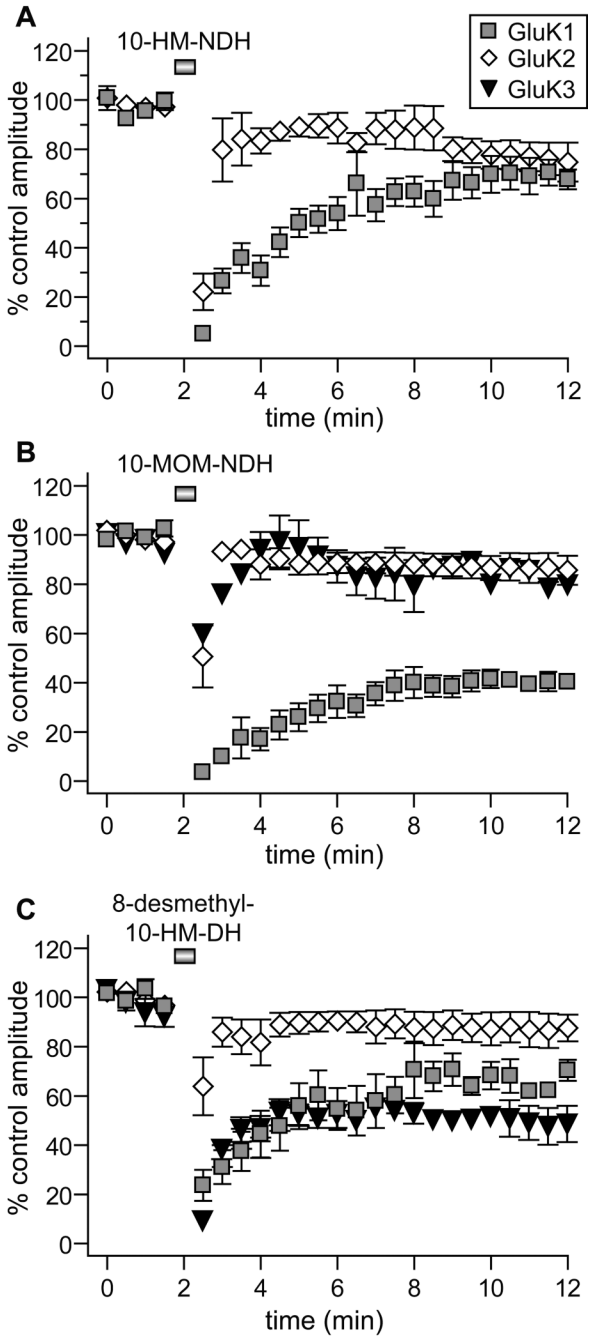

Figure 5.

Time course of recovery of glutamate-evoked currents after application of C10 analogs to kainate receptors. The data represent the normalized amplitude of glutamate-evoked currents (10 mM, 100 ms) relative to the control two-minute period before receptors were exposed to the C10 analogs. (**A**) 10-HM-NDH, (**B**) 10-MOM-NDH, and (**C**) 8-desmethyl-10-HM-DH were applied at 30 μM for 30 sec. Glutamate applications were then resumed at 20 sec intervals for the duration of the experiment. (n = 3–6 at each time point). In each case, GluK1 receptors recovered from analog-induced desensitization at the slowest rate; in the case of 10-MOM-NDH, amplitudes plateaued at a level lower than that of the control. GluK2 receptors recovered

quickly in each case. 10-HM-NDH was not analyzed on GluK3 receptors in (**A**) because this analog showed no affinity for the GluK3 receptor (see Table 1).

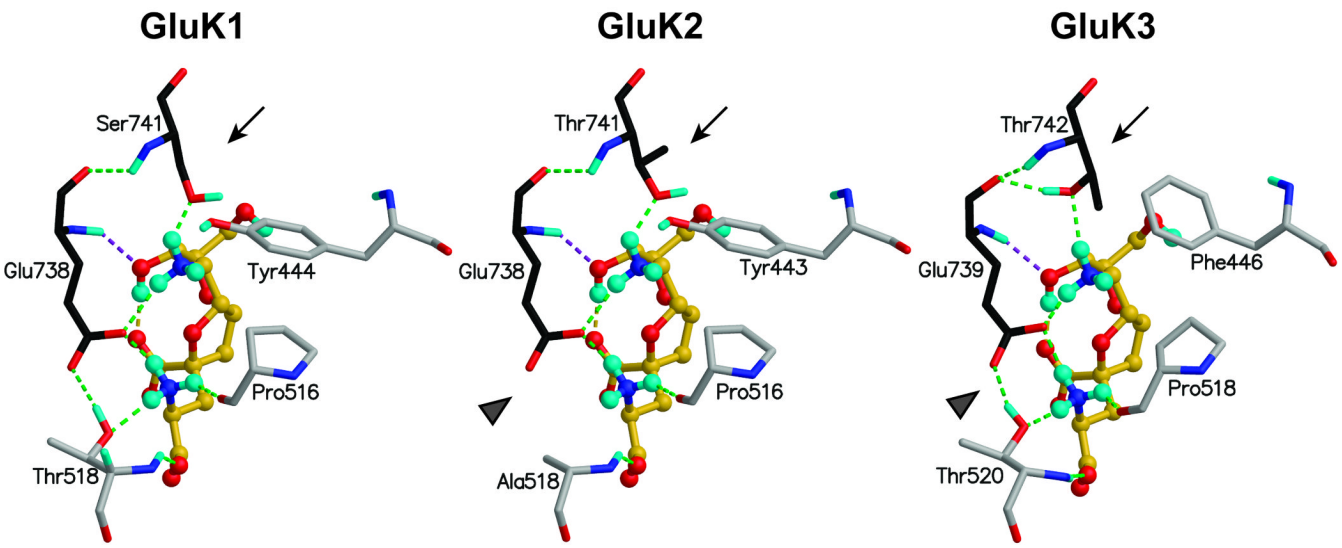

Figure 6.

Binding of 8-desmethyl-10-HM-DH to GluK1-, GluK2-, and GluK3-LBCs derived from MD simulations. Carbon atoms of the amino acid residues in lobe D1 are colored with grey, and from lobe D2 with black. The ligand is shown with an yellow carbon atoms. The hydrogen-bonding interactions are shown with dotted lines. Polar hydrogens (cyan) are shown, while those attached to carbon atoms are left out for clarity. The arrow marks the site of Ser/Thr741-Tyr/Phe444 shift in conformation. The grey arrowhead denotes the position of the differential Ala/Thr518-Glu738 interaction. Numbering in each ligand binding domain is according to position in the full-length subunit.

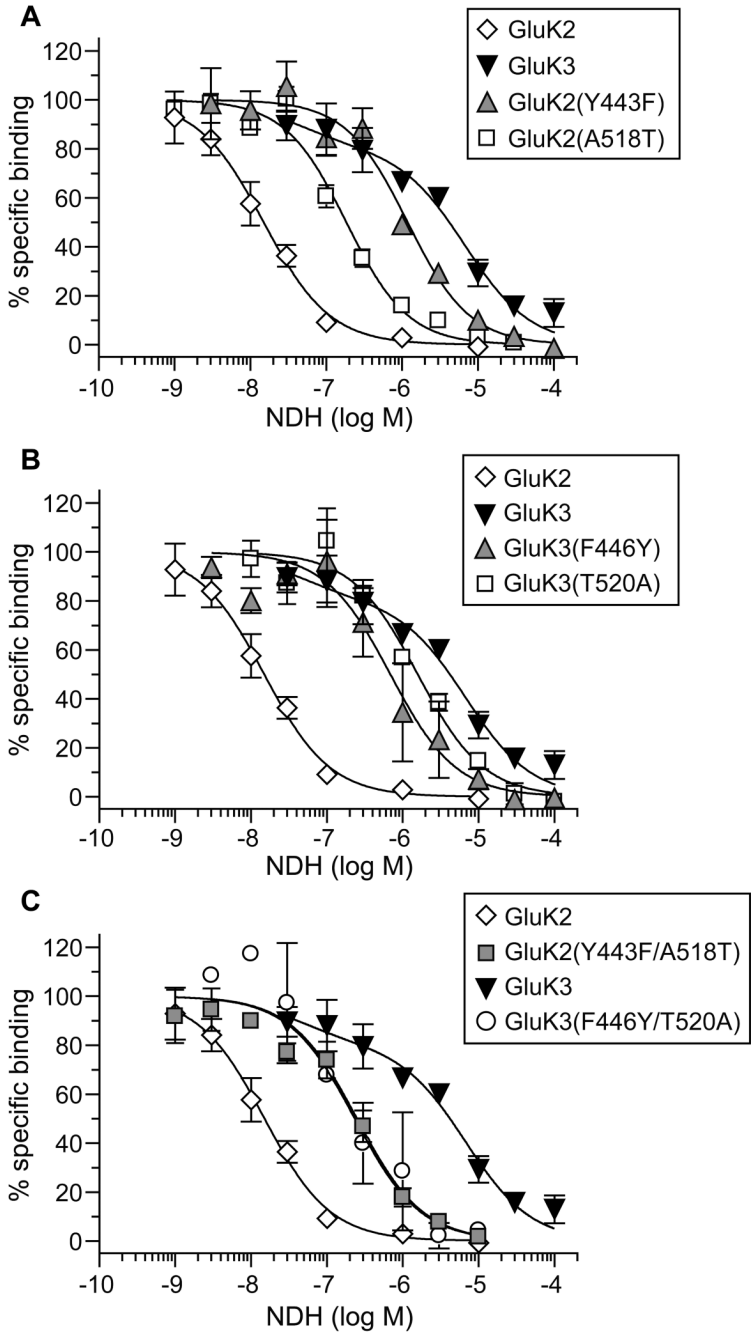

Figure 7.

Analysis of the effect of reciprocal mutations of Tyr443/Phe446 and Ala518/Thr520 on binding to NDH. **A**. Single site mutations in GluK2 of Tyr443 (Y443) to a phenylalanine and Ala518 (A518) to a threonine greatly reduced binding affinity, as evidenced by the substantial shifts to the right in the displacement curves. GluK2 and GluK3 displacement curves are shown for the sake of references in this and the following panels. **B**. Single mutations of Phe446 (F446) and Thr520 (T520) in GluK3 increased affinity for NDH only modestly. **C**. Double reciprocal mutation of residues 443/446 and 518/520 in GluK2 and GluK3 produced receptors with an identical displacement profile intermediate to that of the parent wildtype receptors. K_i values derived from this data are given in the text.

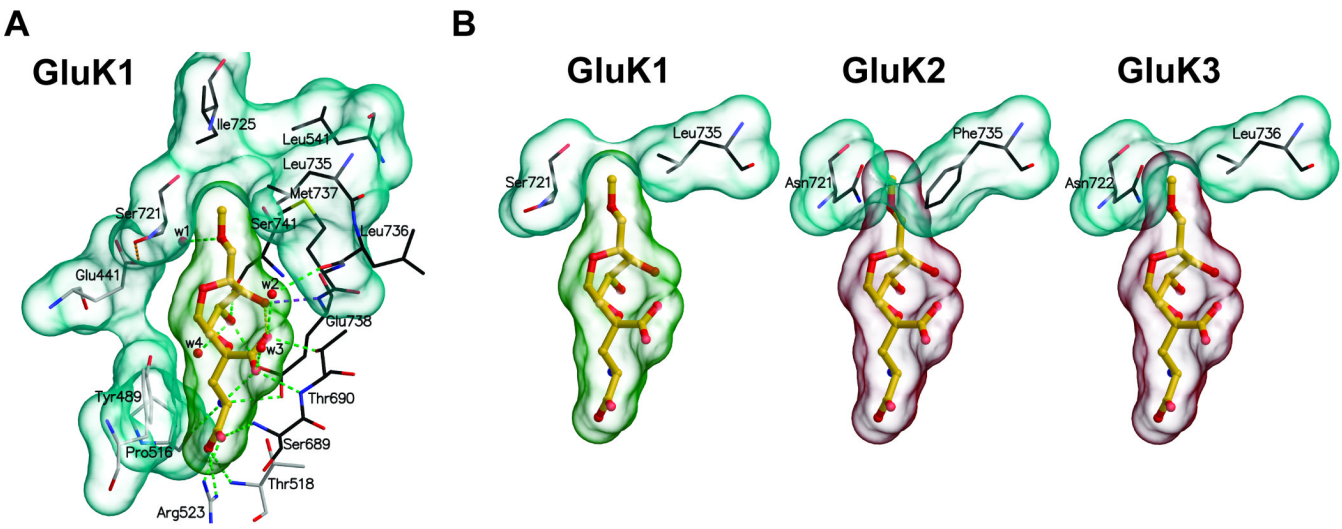

Figure 8.

Binding mode of 10-MOM-NDH to kainate receptors derived from MD simulations with the GluK1 LBC. **A**. The detailed binding configuration for GluK1, demonstrating the compatibility of the C10 substitution for the hydrophobic niche in the binding pocket. **B**. The predicted effect of sequence differences in GluK1–3 at positions 721 and 735 in shaping the binding pocket and complementarity for C10 functional groups. Carbon atoms of the amino acid residues in D1 are colored with grey, and from D2 with black. The hydrogen bonding interactions are shown with dotted lines (see legend for Fig. 6 for additional information).

Neuropharmacology. Author manuscript; available in PMC 2011 March 1.

Table 1

Ki values for displacement of [^{3}H]kainate (GluK1–3) or [^{3}H]AMPA (GluA1–2) by parent compounds and C10-substituted analogs of DH on kainate and AMPA receptor subunits expressed in HEK-293-T/17 cells. Mean values were calculated using K_d and IC_{50} values with the Cheng-Prusoff equation (as described in the Methods). IC_{50} values were obtained using a one-site competition fit, with the exception of NDH binding to GluK3 subunits, which was best-fit with a two-site competition model. Values are given in nM for kainate receptor subunits and μM for AMPA receptor subunits. 95% confidence intervals and number of measures are as described in the text.

	GluK1	GluK2	GluK3	GluK5	GluA1	GluA2
	nM	*nM*	*nM*	*nM*	μM	μM
DH	0.5	1.3	5.4	4300	N.D.	N.D.
NDH	7.7	8.4	3,005	680	N.D.	N.D.
10-HM-NDH	59	834	>10,000	>10,000	>10	~10
10-MOM-NDH	10	2,426	14,530	>10,000	>10	>10
8-desmethyl-10-HM-DH	7.2	929	397	>10,000	>10	>10